Growth-rate dependent global effects on gene expression in bacteria

Stefan Klumpp, Zhongge Zhang, and Terence Hwa

— Supporting Information —

Manuscript information:

5 Supporting Figures (6 pages)

3 Supporting Tables (3 pages)

Supporting Text: Detailed description of circuit models and supplemental experimental procedures (30 pages)

References (3 pages)

SUPPORTING TABLES AND FIGURES

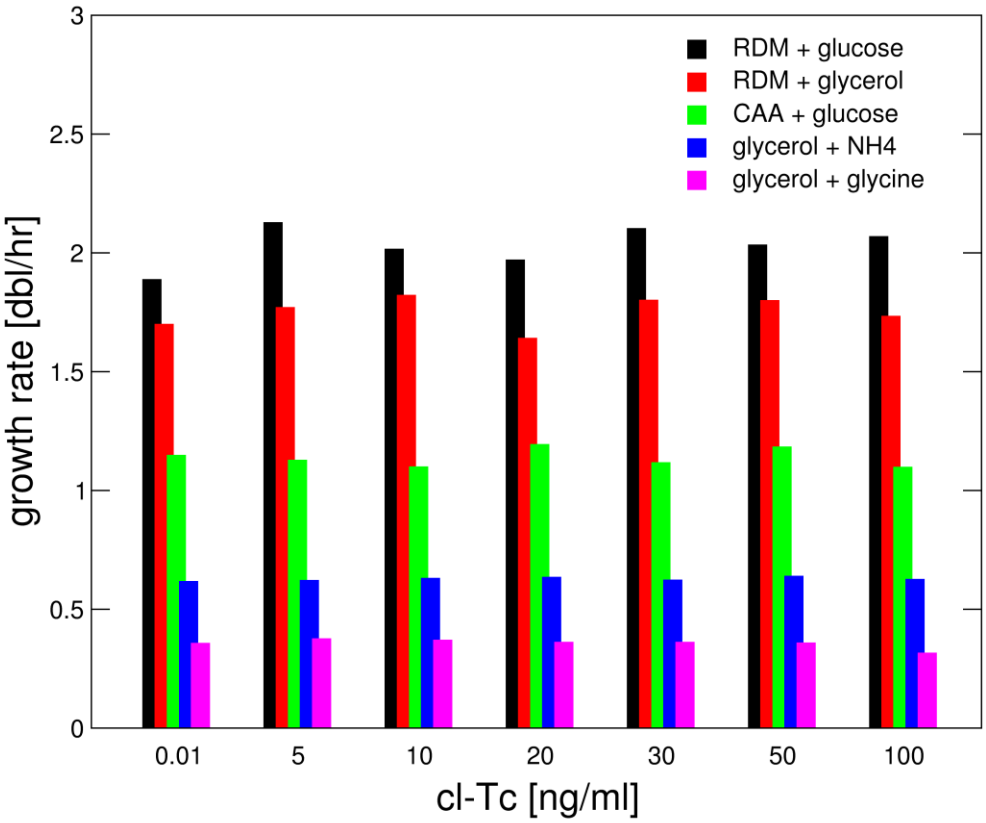

Figure S1: Growth rate at different inducer concentrations. The growth rate of strain EQ38 is shown for different concentrations of the inducer cl-Tc and different growth media.

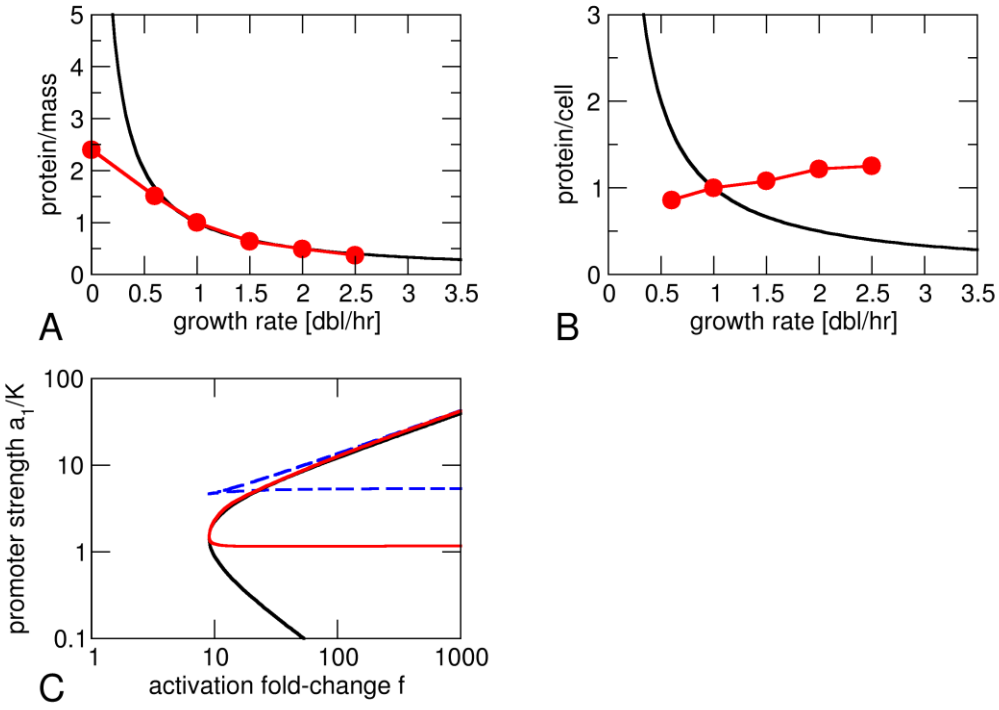

Figure S2: Growth-rate dependent effects in a dilution-only model. Predictions of our model with several growth rate dependent parameters (red) are compared to the corresponding predictions of a model, where growth only affects protein dilution (black). (A) A dilution-only model is expected to predict the concentration of a constitutively expressed protein well for growth rates >0.6 dbl/hr, but to overestimate it strongly for slower growth rates, where it predicts a diverging protein concentration. In contrast, Fig. 3 indicates that this concentration approaches a finite value for growth rates approaching zero. Here this value (red circle at zero growth rate) is estimated by extrapolating the prediction of our model using the linear relation of protein concentration per total protein (Fig. 3B) together with an extrapolation of total protein per mass (Bremer and Dennis, 1996). (B) Since dilution-only models do not incorporate the growth-rate dependence of the cell volume (or cell mass), they predict the same growth-rate dependence for protein/cell as for protein/mass, in contrast to our model. (C) Dilution-only models overestimate the effect of growth feedback: The region of bistability for an autoactivator that reduces growth (with a_1/a_μ=0.2, μ_0=2.5 dbl/hr, compare Fig. S3) is much bigger in

the dilution-only model (black) than in our model (red). For comparison, the dashed blue line indicates the bistable region in the absence of growth reduction.

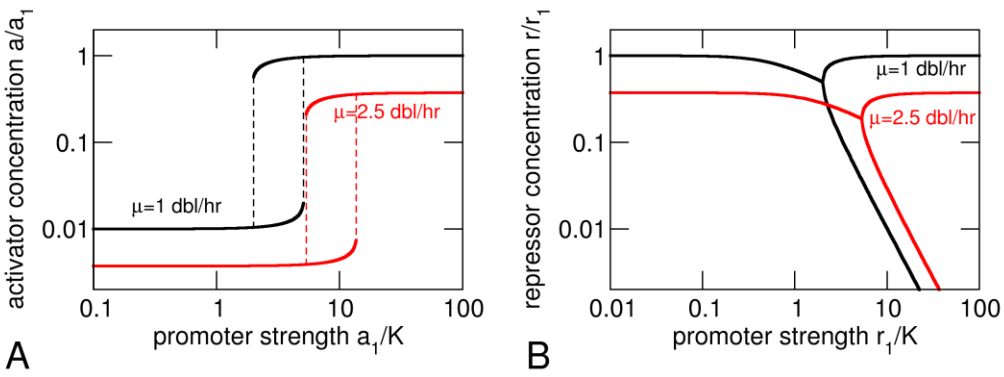

Figure S3: Bistability in the autoactivator and toggle switch circuits. Concentrations of the activator (A) or the repressors (B) as functions of the respective 'promoter strength' a_1/K or r_1/K (taken to be the same for both promoters in the toggle switch) at growth rates of 1 doubling per hour (black) and 2.5 doublings/hour (red). The parameters are f=100 (A) and n=2 (A and B).

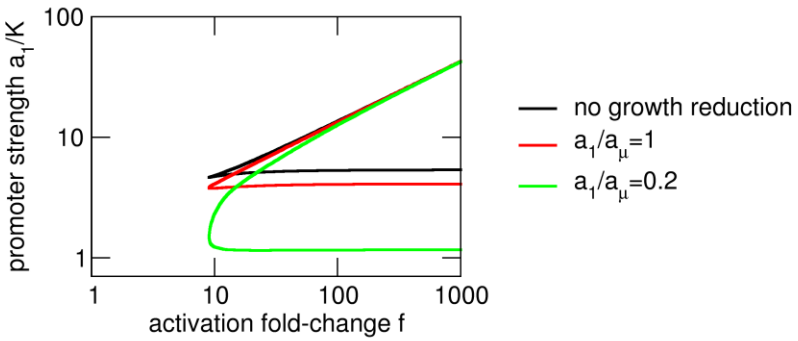

Figure S4: Combined effect of positive feedback through growth and through regulation in an autoactivator circuit. The lines plot the perimeter of the parameter range for bistability as function of the promoter strength and the activation fold-change. The black curve shows the case where the activator concentration does not affect the growth rate, the data shown are the same as the red curve in Fig. 6A (Hill coefficient n=2). The red and green lines show the case of non-cooperative growth reduction by the same activator (or, equivalently, by any protein that is co-regulated with this activator) with different thresholds (a_μ) for growth reduction. Comparison of the three curves shows that growth reduction by the autoactivator can substantially enlarge the range for bistability.

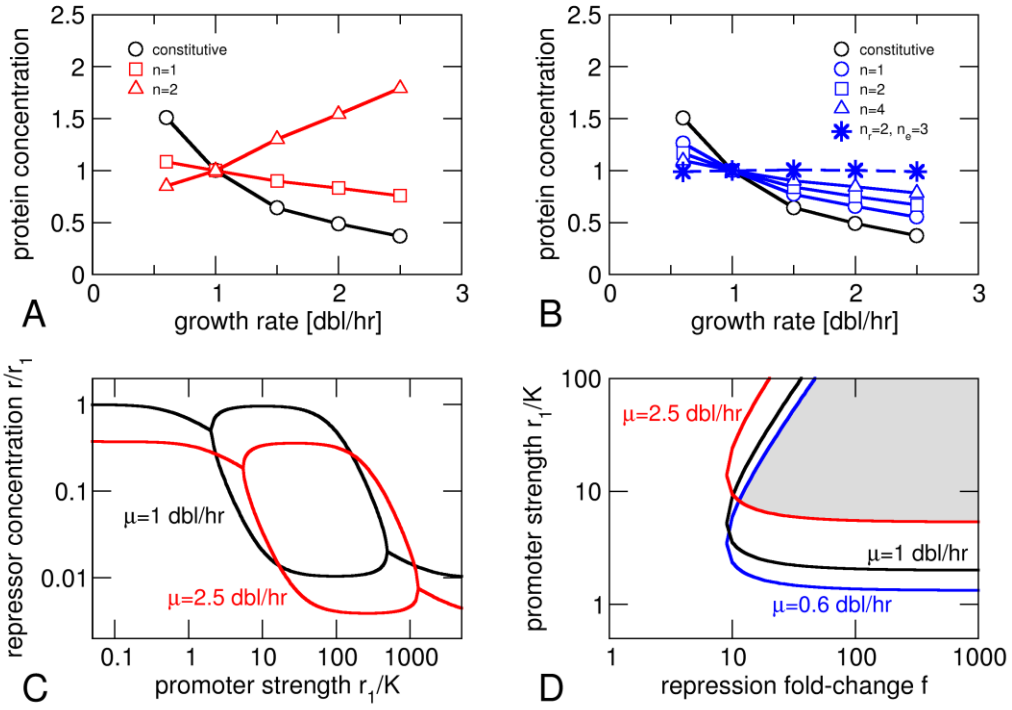

Figure S5: Repression with a basal level of expression. (A) Concentration of a protein under negative regulation by a constitutively expressed repressor as in Fig. 4A, but with a repression fold-change f=1000 (r_1/K=10). (A) Growth rate dependence of a gene controlled by negative autoregulation as in Fig. 5B, but again with f=1000. The results are very similar to those without the basal level. (C) Toggle switch with repressors with a basal expression level: Concentration of the repressors as function of the promoter strength, as in Fig. S3 B, but with f=100. In contrast to the case without basal level, bistability is lost for very strong promoters. (D) The corresponding parameter range for bistability (for two repressors characterized by the same parameters and n=2) indicates a large region where bistability persists over a wide range of growth rates (grey area), considerably larger than in the case of an autoactivator (Fig. 6A).

Table S1: Growth-rate dependent parameters

Parameter	Symbol	Growth rate μ [dbl/hr]					Notes and references
		0.6	1.0	1.5	2.0	2.5	
Transcription rate per gene (relative)	α_m	0.65	1	1.31	1.49	1.51	Calculated from free RNA polymerase concentration (Klumpp and Hwa, 2008), in agreement with measured transcription rates for several constitutive promoters (Liang et al., 1999a)
Gene copy number	*g*	1.6	1.8	2.3	3.0	3.8	average gene (Bremer and Dennis, 1996)
		1.96	2.43	3.36	4.70	6.54	gene at replication origin (*m'*=0), calculated using the Cooper-Helmstetter relation(*)
		1.55	1.82	2.28	2.86	3.56	Gene halfway between replication origin and terminus (*m'*=0.5) (*)
		1.23	1.37	1.54	1.74	1.94	Gene at replication terminus (m'=1) (*)
		39	41	46	51	56	Gene on plasmid pBR322 (Lin-Chao and Bremer, 1986)
		8.5	4.8	3.3	2.6	1.3	Gene on plasmid R1 (Engberg and Nordstrom, 1975)
C period of cell cycle [min]	*C*	67	50	45	43	42	(Bremer and Dennis, 1996), needed for the calculation of *g* for chromosomal genes
D period of cell cycle [min]	*D*	30	27	25	24	23	
mRNA lifetime [min]	$\tau_m=1/\beta_m$	1.9	2.0	2.1	2.2	2.3	(Liang et al., 1999b; Liang et al., 2000) data for lacZ, values for 0.6 and 3 dbl/hr are measured; other values are interpolated
Translation rate (relative)	α_p	0.97	1	0.94	0.94	0.90	(Liang et al., 2000)
Protein dilution rate [10^{-3} min^{-1}]	β_p	6.9	11.5	17.3	23.1	28.9	$\beta_p=\mu \ln 2$
Mass per cell [OD_{460} units/10^9 cells]	M_C	0.85	1.49	2.5	3.7	5.0	(Bremer and Dennis, 1996)

(*) The gene copy number is given by $g=2^{\mu[C(1-m')+D)]}$ with *m'* denoting the position on the chromosome (distance to replication origin relative to the distance between the replication origin and terminus, i.e. *m'*=0 corresponds to the replication origin and *m'*=1 to the replication terminus). *C* and *D* are the durations of the C and D period of the cell cycle.

Table S2. Strains and plasmids used in this study

Strains	**Genotype or description**	**Reference or source**
EQ1	Wild type *E. coli* K12 strain MG1655	F. R. Blattner
EQ42	Δ*lacY*	EQ1; this study
EQ43	Δ*lacY*, *bla*:P_{con}-*tetR* at the *attB* site	EQ42; this study
EQ44	Δ*lacY*, *bla*:$P_{LTet\text{-}O1}$-*tetR* at the *attB* site	EQ42; this study
EQ45	Δ*lacY*, *bla*:$P_{Llac\text{-}O1}$-*dnxylR* at the *attB* site	EQ42; this study
EQ37	Δ*lacY*, Δ*lacI*, *km*:*rrnB*T:$P_{LTet\text{-}O1}$-*lacZ* at the *lac* locus,	EQ42; this study
EQ48	Δ*lacY*, Δ*lacI*, *km*:P*u*-*lacZ* at the *lac* locus,	EQ42; this study
EQ38	Δ*lacY*, Δ*lacI*, *km*:*rrnB*T:$P_{LTet\text{-}O1}$-*lacZ* at the *lac* locus, *bla*:P_{con}-*tetR* at the *attB* site	EQ37; this study
EQ39	Δ*lacY*, Δ*lacI*, *km*:*rrnB*T:$P_{LTet\text{-}O1}$-*lacZ* at the *lac* locus, *bla*:$P_{LTet\text{-}O1}$-*tetR* at the *attB* site	EQ37; this study
EQ40	Δ*lacY*, Δ*lacI*, *km*:P*u*-*lacZ* at the *lac* locus, *bla*:$P_{Llac\text{-}O1}$-*dnxylR* at the *attB* site	EQ45; this study
Plasmids		
pgalK	Ap^r, pUC *ori*, *galK*	Warming *et al*., 2005
pZA31B-*luc*	Cm^r, p15A *ori*, $P_{LTet\text{-}O1}$-*luc*	Lutz & Bujard, 1997; Levine *et al.*, 2007
pZE12G	Ap^r, colEI *ori*, $P_{Llac\text{-}O1}$-*gfpmut3b*	Levine *et al.*, 2007
pKD13	Km^r, R6K *ori*	Datsenko & Wanner, 2000
pKD13-P*tet*	Km^r, R6K *ori*, $P_{LTet\text{-}O1}$	This study
pKD13-*rrnB*T:P*tet*	Km^r, R6K *ori*, *rrnB*T:$P_{LTet\text{-}O1}$	This study
pKD13-P*u*	pKD13 carrying P*u*	This study
pZSin-4	Sp^r, sc101 *ori*, Pcon-*tetR*, *lacI*q	Lutz & Bujard, 1997
pLDR10	Cm^r, Ap^r, colEI *ori*, *attP*	Diederich *et al*., 1992
pLDR10Pcon-*tetR*	pLDR10 carrying Pcon-*tetR*	This study
pZA31-*tetR*	pZA31 carrying $P_{LTet\text{-}O1}$-*tetR*	This study
pLDR10P*tet*-*tetR*	pLDR10 carrying $P_{LTet\text{-}O1}$-*tetR*	This study
pZE12-*dnxylR*	pZE12 carrying $P_{Llac\text{-}O1}$-*dnxylR*	This study
pLDR10P*lac*-*dnxylR*	pLDR10 carrying $P_{Llac\text{-}O1}$-*dnxylR*	This study

Table S3. Oligonucleotides used in this study

Name	Sequence	Use
GalK1-P1	ccaacgcatttggctaccctgccactcacaccattcaggcgcctggtgtaggctggagctgcttc	*galK* deletion
GalK2-P2	agtctctttaatacctgtttttgcttcatattgttcagcgacagccatatgaatatcctccttag	*galK* deletion
GalK1-lacY1	tcatgggagcctacttcccgtttttcccgatttggctacatgacatcaacctgttgacaattaatcatcggc	*galK* substitution for *lacY*
GalK2-lacY2	agcgtgaacacggaaattaaggtgaagcccagcgccaccagacccagcactcagcactgtcctgctcctta	*galK* substitution for *lacY*
Del-galK-F	tcatgggagcctacttcccgtttttcccgatttggctacatgacatcaacgtgctgggtctggtggcgctggcttcaccttaatttccgtgttcacgct	Deletion of *galK* in the *lacY* locus
Del-galK-R	agcgtgaacacggaaattaaggtgaagcccagcgccaccagacccagcacgttgatgtcatgtagccaaatcgggaaaaacgggaagtaggctcccatga	Deletion of *galK* in the *lacY* locus
Ptet-Sal	aaagtcgacgttggaacctcttacgtgccgatc	Cloning P*tet* into pKD13
Ptet-Bam	aaaggatcctttctcctctttaatgaattcg	Cloning P*tet* into pKD13
rrnBT1-Sal	atagtcgacgatggtagtgtggggtctcc	Cloning *rrnB*T upstream of P*tet* in pKD13
rrnBT1-Xho	aatctcgagacgcaaaaaggccatccgtcag	Cloning *rrnB*T upstream of P*tet* in pKD13
Pu-Sal	aaagtcgacccttcgtcttcacctcg	Cloning P*u* into pKD13
Pu-Bam	aaaggatccgattaagttgggtaacgccagg	Cloning P*u* into pKD13
Plac-Sal	aaagtcgacccttcgtcttcacctcg	Cloning P*lac* into pKD13
Plac-Bam	aaaggatccgattaagttgggtaacgccagg	Cloning P*lac* into pKD13
dnxylR-Kpn	aaaggtaccatggagttcctgaagcagtacgatgggcagtattacgg	Cloning *dnxylR* into pZE12
dnxylR-Xba	atatctagactatcggcccattgctttcacagataagc	Cloning *dnxylR* into pZE12
PlacdnxylR-Sac	aaagagctccttcacctcgagaattgtgagcgg	Cloning P*lac-dnxylR* into pLDR10
PlacdnxylR-Bam	aaaggatccataccgctcgccgcagccgaac	Cloning P*lac-dnxylR* into pLDR10
lacI-kpn	aaaggtaccatgaaaccagtaacgttatacg	Cloning *lacI* into pZA31
lacI-Bam	aaaggatcctcactgcccgctttccagtcgg	Cloning *lacI* into pZA31
Ptet1-P1	gcatttacgttgacaccatcgaatggcgcaaaacctttcgcggtatgtgtaggctggagctgcttc	Chromosomal substitution of *rrnB*T:P*tet* for *lacI* and P*lacZYA*
Ptet2-P2	cgttgtaaaacgacggccagtgaatccgtaatcatggtcatagctgttttctcctctttaatgaattcgg	Chromosomal substitution of *rrnB*T:P*tet* for *lacI* and P*lacZYA*
Pu1n-P1n	gcatttacgttgacaccatcgaatggcgcaaaacctttcgcggtatgtgtaggctggagctgcttc	Chromosomal substitution of P*u* for *lacI* and P*lacZYA*
Pu2-P2	ggtaacgccagggttttcccagtcac	Chromosomal substitution of P*u* for *lacI* and P*lacZYA*

SUPPORTING TEXT

Detailed description of the circuit models

Constitutive expression

Gene expression is modeled by two equations describing the dynamics of mRNA and protein product, respectively:

$$\dot{M} = \alpha_m g - \beta_m M \quad \text{(S1)}$$

$$\dot{P} = \alpha_p M - \beta_p P \quad \text{(S2)}$$

In these equations, M and P denote the amounts of mRNA transcript and protein product of a constitutively expressed gene in terms of numbers of molecules per cell. α_m is the transcription rate per gene copy, g is the gene copy number per cell, α_p is the translation rate (per transcript) and β_m and β_p are the degradation rates of the transcript and the protein, respectively. In the steady state, we obtain $M=\alpha_m g/\beta_m$ and $P=\alpha_m\alpha_p g/(\beta_m\beta_p)$ for the amounts (in molecules per cell) of mRNA and protein and $m=M/V=\alpha_m g/(\beta_m V)$ and $p=P/V=\alpha_m\alpha_p g/(\beta_m\beta_p V)$ for the corresponding concentrations. Throughout the paper, we use data for the mass per cell M_C as measured by optical density rather than the volume V to calculate concentrations, since the quantities are proportional and mass per cell is more easily measured (see below).

We take mRNA to be unstable with lifetimes short compared to the bacterial doubling time, and take protein to be stable with lifetimes much longer than the doubling time, as it is typically the case in bacteria. This assumption means that dilution of the cellular mRNA content due to cell growth and division can be neglected. Furthermore it allows us to identify protein degradation with dilution by growth, so that $\beta_p=\mu \ln 2$. Since mRNA

dynamics is rapid with typical lifetimes of a few minutes (Bernstein et al., 2002), we can also summarize Eqs. (S1) and (S2) into

$$\dot{P} = \alpha_m \alpha_p g / \beta_m - \beta_p P. \tag{S3}$$

This equation can be rewritten in terms of the protein concentration $p=P/V$,

$$\dot{p} = \alpha_m \alpha_p g /(\beta_m V) - \beta_p p. \tag{S4}$$

The solution of this equation, which describes the growth-rate dependence of the protein concentration for a constitutively expressed gene, is given by Eq. (1) in the main text. For the following discussion of regulated genes, we scale time by the dilution rate β_p in order to summarize all growth-rate-dependent factors in one function $F(\mu)$,

$$\dot{p} = \alpha_m \alpha_p g /(\beta_m \beta_p V) - p = p_1 F(\mu) - p. \tag{S5}$$

Here we have normalized $F(\mu)$ to the value at 1 doubling per hour, i.e., $F(\mu=1) = 1$; it is the black curve plotted in Fig. 2D. The parameter p_1, which numerically corresponds to the concentration of the constitutively expressed protein at a growth rate of 1 doubling per hour, is used throughout the model to characterize the degree of basal expression. We refer to it as the promoter strength even though it can also be changed by the translational efficiency of the transcript through the quality of the ribosomal binding site.

Growth-rate dependence of cellular parameters

The level of expression of a constitutively expressed gene is growth-rate dependent, because several parameters of gene expression are dependent on the growth rate. We have collected the growth-rate dependence of all the parameters of Eq. (S4) or, equivalently, of Eq. (1) from the experimental literature, as described in the main text and shown in Fig. 1. Before we proceed to the discussion of regulated genes and genetic

circuits, we make a few additional comments on some aspects of these growth-rate dependences.

Growth-rate dependence of mRNA stability:

As described in the main text, mRNA lifetimes are quite independent of the cellular growth rate generally, although there are examples of specific transcripts for which the lifetime is regulated in a growth-rate dependent fashion (Nilsson et al., 1984). In our model, the independence of growth rate is taken as an experimental fact and used as an input. Here we speculate on the possible origin of this finding.

Several observations indicate that the growth-rate independence of transcript stability likely arises from the regulation of RNase E, the main enzyme mediating mRNA decay in E. coli (Kushner, 2007). The level of RNase E is controlled by negative autoregulation: RNase E cleaves its own transcript (Jain and Belasco, 1995; Mudd and Higgins, 1993), and the lifetime of the RNase E mRNA is unusually sensitive to changes in the cellular RNase E level, compared to other transcripts (Jain and Belasco, 1995). As a consequence, RNase E levels are downregulated in response to an excess of RNase E (Jain and Belasco, 1995; Mudd and Higgins, 1993) and upregulated in response to shortage (Jain et al., 2002). Negative autoregulation in general results in constant protein levels and our analysis indicates that this level is also approximately independent of growth rate (Fig. 5B). With the caveat that the autoregulation of RNase E may be more complex than our model, we would thus expect an approximately constant RNA degradation activity and thus growth-rate independent mRNA lifetimes. The latter expectation can be viewed as a check of the consistency of our model.

Furthermore, RNase E appears to be present in the cell in excess, at least in rich medium (Ow et al., 2002): The cellular level of RNase E can be reduced strongly with only a weak effect on general mRNA stability. This indicates that even if the level of RNase E changes somewhat as a function of growth rate, one could still expect mRNA lifetimes (or degradation rates) to be rather independent of growth rate.

Growth-rate dependence of the ranslation rate:

The translation rate per message is approximately independent of growth rate (Fig. 1D). This is surprising because the translation rate should reflect the availability of ribosomes and the ribosome content of the cell is known to increase strongly at fast growth (Bremer and Dennis, 1996). A likely explanation of the constant translation rate is that the concentration of *free* ribosomes, which are available to initiate translation, is approximately constant over this range of growth rates (Liang et al., 2000). The constant translation rate thus suggests the intriguing possibility that a feedback mechanism acts on the *free* ribosome concentration in order to keep it constant as opposed to a feedback regulation of the total ribosome concentration. Feedback regulation of ribosome synthesis by the free ribosomes has been proposed long ago (Jinks-Robertson et al., 1983), but has generally been dismissed, because it was not consistent with the observed requirement of initiation factors for feedback regulation (Cole et al., 1987). A feedback mechanism that is consistent with this observation is however possible, provided that free ribosomes are sensed through their ability to initiate translation, e.g. via the translation rate of a protein or peptide signal, rather than being sensed directly.

Burstiness of gene expression:

A quantity closely related to the translation rate is the average number of proteins made per mRNA molecule, $b=\alpha_p/\beta_m$, the product of translation rate (α_p) and mRNA lifetime ($1/\beta_m$). The quantity *b* describes the amplification of gene expression by translation and is often referred to as "burstiness", since proteins are synthesized in bursts of *b* molecules if transcription events are infrequent (Cai et al., 2006; Ozbudak et al., 2002). As both the translation rate and the mRNA lifetime are approximately independent of growth rate for constitutively expressed genes (Fig. 1D and 1E), the same is true for the burstiness *b*. More general, based on the growth-rate dependence of the parameter shown in Fig. 1, we expect constant burstiness not only for constitutively expressed genes, but for all genes that are not subject to specific post-transcriptional regulation.

There is an apparent discrepancy between the constant burstiness for a constitutively expressed gene and the average number of proteins made per mRNA, which has been reported to increase from ~20 at 0.6 doublings/hour to ~100 at 2.5 doublings/hour (Bremer and Dennis, 1996). This apparent discrepancy can however be resolved by noting that the latter average is taken over all proteins and all transcripts in the cell. The increase in burstiness at fast growth thus reflects the different composition of the transcriptome at different growth rates (e.g. a higher content of proteins with larger burstiness). In addition, this average also includes post-transcriptionally regulated genes. In particular the burstiness of ribosomal proteins is expected to increase strongly at fast growth, where their expression is upregulated at the translational level (Keener and Nomura, 1996). Since ribosomal proteins constitute up to ~30 percent of the total protein content of the cell, their increased burstiness is expected to have a strong effect on the total average number of proteins per mRNA.

Cell volume, cell mass, and total protein per cell:

One ingredient of our analysis is the growth rate dependence of the cell volume. In our analysis we use cell mass (or alternatively, total protein per cell) as measures of cell volume, since these are commonly used as normalizations to express cellular concentrations. We consider these three quantities as essentially equivalent measures of the size of a cell, at least for cells growing exponentially in batch culture under constant osmolarity. In the following we review the experimental evidence on which this assumption is based.

Cell volume, determined either from analysis of electron microscopy images or using a Coulter Channelyser, has been found to exhibit the same functional dependence on growth rate as cell mass, which is determined from optical density measurement and cell count (Donachie and Robinson, 1987; Nanninga and Woldringh, 1985). [That optical density measurements reflect cellular mass is shown by the proportionality between optical density and either dry weight or the summed mass of protein+DNA+RNA,

measured for different growth media (Brunschede et al., 1977; Dennis and Bremer, 1974; Schaechter et al., 1958). This proportionality is valid for sufficiently low cell densities, corrections are necessary for higher cell densities (Bipatnath et al., 1998; Lawrence and Maier, 1977).] Likewise, direct measurements of the density (i.e. the ratio of mass and volume) of *E. coli* cells using centrifugation showed little dependence on growth rate, with at most a very weak increase of <1% at fast growth (Nanninga and Woldringh, 1985; Woldringh et al., 1981), which also indicates that cell mass and cell volume have the same growth-rate dependence. A growth-rate independent density is also suggested by studies on macromolecular crowding, which exhibited only small changes between exponentially growing and stationary cells (Zimmerman and Trach, 1991) and by comparison of the diffusion of GFP in the cytoplasm at different growth rates, which exhibits the same diffusion coefficient (Elf et al., 2007; Elowitz et al., 1999; see also the discussion in Klumpp and Hwa, 2008). We note however that macromolecular crowding increases under osmotic stress (Cayley and Record, 2004), so that the relations between optical density, mass and volume have to be reconsidered if cells are grown in media with unusually high or low osmolarity.

As an alternative to total mass per cell, one can also use total protein per cell to express cellular concentrations. This normalization thus expresses concentrations as proteome fractions, which is well suited for interpretation in terms of the partitioning of cellular resources (Maaløe, 1979; Scott et al., 2009). However, the ratio of protein/mass increases slightly at slow growth (Bremer and Dennis, 1996), so that the growth rate dependence of a constitutively expressed protein is slightly weaker if its concentration is expressed per total protein rather than per mass (compare Figures 3A and B).

Repression and activation by constitutively expressed regulators

Repression by a constitutively expressed repressor is described by two equations, one for the repressor concentration *r* and one for the protein concentration *e* of the repressed gene

$$\dot{r} = r_1 F_r(\mu) - r$$
$$\dot{e} = e_1 F_e(\mu) R(r/K) - e$$

(S6)

(S7)

Here we have used indices r and e in the growth rate function $F(\mu)$ to indicate that the growth rate effect on the two genes may be different, e.g., due to different locations of the genes on the chromosome (through positional dependence of the gene copy number). While this difference is relatively small for chromosomal genes, it may be quite large if one of the genes is encoded on a plasmid. The parameter r_1 plays exactly the same role as p_1 does for constitutive expression, i.e., it characterizes the strength of the promoter driving the repressor gene. The parameter e_1 plays a similar role. With the regulation function R defined such that $R(0)=1$ (see below), e_1 gives the concentration of the protein E at a growth rate of 1 doubling per hour at maximal expression, i.e. in the absence of repression. Hence, e_1 characterizes the strength of the target promoter.

Repression is described quantitatively by the repression function (Bintu et al., 2005)

$$R(r/K) = \frac{1}{1+(r/K)^n}. \tag{S8}$$

This function has two parameters, the Hill coefficient n, which characterizes the cooperativity of repression, and the repressor concentration scale K, which characterizes the repression "threshold" and corresponds to the repressor concentration at which expression is reduced to half its maximal value. We note that for this form of the repression function, which is used throughout the main text, sufficiently high repressor concentrations lead to complete repression of the gene, i.e. with no protein synthesis. The case that there is a low basal level of expression even in the presence of saturating repressor concentrations is discussed below, where we show that presence or absence of such a basal level lead to very similar growth-rate dependencies. The repression function R exhibits two different regimes: If the repressor concentration is small compared to K, repression is negligible and we have $R\sim1$, which corresponds to constitutive expression at the maximal level. For larger repressor concentrations such that $(r/K)^n$ is large compared to 1, we have the repressing regime with $R\sim(K/r)^n$. In this regime, the growth rate

dependence of a repressed gene differs from that of a constitutively expressed gene. For (r/K)~1, we obtain a crossover between constitutive and repressed behavior.

In the steady state, the repressor concentration is given by $r=r_1F_r(\mu)$ and the concentration of the repressed protein by $e=e_1F_e(\mu)R(r_1F_r(\mu)/K)$. In the repressing regime, the latter expression can be approximated by

$$e = e_1 \frac{F_e(\mu)}{(r_1/K)^n F_r(\mu)^n} \approx \frac{e_1}{(r_1/K)^n} F(\mu)^{-n+1}. \quad \text{(S9)}$$

Here the last approximation assumes that the two genes have similar growth rate dependence, i.e. that they are located in close proximity on the genome. This approximation shows that the protein concentration for a gene repressed by a constitutively expressed repressor without cooperativity (Hill coefficient n=1) is approximately independent of growth rate. We note that this approximation is valid if there the repressor is in excess compared to the repression threshold K at all growth rates, i.e. if r_1 is large compared to K (e.g. for r_1/K=100). For r_1/K=10, as shown in Fig. 4A, there is a weak inverse dependence on growth rate. This dependence becomes more and more similar to the constitutive case if r_1/K is decreased further. For cooperative repression (n>1), we obtain an increase of the protein concentration with increasing growth rate, because $F(\mu)$, which decreases with increasing μ, now appears in the denominator. Again this dependence becomes weaker if r_1/K is decreased. For (r_1/K)~1, the growth rate dependence is generally weak and can exhibit a maximum, increasing at slow growth as for a repressed gene and decreasing at fast growth as in the constitutive case. This reflects a 'crossover' between a situation where the repressor concentration is in excess over K at slow growth, and hence E behaves as a repressed gene, and an almost constitutive situation, where the repression level is low compared to K and repression becomes negligible at fast growth.

Simple activation is described in an analogous fashion. The repressor concentration r is replaced by the activator concentration a, the repressor promoter strength r_1 by the

activator promoter strength a_1, and the repression function $R(r/K)$ by an activation function $A(a/K)$, given by (Bintu et al., 2005)

$$A(a/K) = \frac{\frac{1}{f} + (a/K)^n}{1 + (a/K)^n}, \tag{S10}$$

with $A(a \to \infty) = 1$. The new parameter f describes the fold-change of activation, i.e. the ratio between the fully activated expression level and the basal expression level in the absence of the activator. The concentration of the positively controlled protein is then given by

$$e = e_1 F_e(\mu) A(a_1 F_a(\mu)/K). \tag{S11}$$

All parameters are completely analogous to the case of negative regulation, but we note that e_1 again denotes the concentration of E at 1 doubling per hour and maximal expression, i.e. at full activation.

Autorepression and repression by an autorepressor

Autorepression is described by

$$\dot{r} = r_1 F(\mu) R(r/K) - r \tag{S12}$$

and the growth-rate dependence of the steady-state concentration of the repressor r is given by the solution of

$$r/r_1 = F(\mu) R(r/K), \tag{S13}$$

which we determine numerically to obtain to results shown in Fig. 5B. Provided that the resulting repressor concentration is sufficiently high, so that the gene is actually repressed, an approximate analytical solution of this equation leads to

$$r \approx K\left[\frac{r_1}{K}F(\mu)\right]^{1/(n+1)}. \tag{S14}$$

This result indicates that the growth rate dependence is weaker than for constitutive expression and that the effect of growth rate becomes weaker for higher cooperativity. Complete independence of growth rate is obtained in the limit of infinitely cooperative repression.

A gene that is under negative control by the autoregulated repressor is described by

$$\dot{r} = r_1 F(\mu) R(r/K_r) - 1 \tag{S15}$$

$$\dot{e} = e_1 F(\mu) R(r/K_e) - 1, \tag{S16}$$

where the repression functions R_r and R_e may have different Hill coefficients (n_r and n_e) and repression threshold K_r and K_e. The concentration of the repressor is given by Eq. (S13) or (S14) (with indices *e* added to the repression parameters) and the concentration of the protein product of the repressed gene E is given by $e=e_1F_e(\mu)R_e(r/K_e)$. If both repression functions have the same parameters, the repressed gene E has exactly the same growth-rate dependence as the repressor. This situation applies, e.g., to the case where both genes belong to the same operon. If the parameters of the two genes differ, the results can be more complex. If repression of both genes is in the regime of actual repression, we can again find an approximate solution,

$$e \approx e_1 \frac{F_e(\mu)}{\left[\frac{r_1}{K_r}F_r(\mu)\right]^{\frac{n_e}{n_r+1}}\left[\frac{K_r}{K_e}\right]^{n_e}} \propto F(\mu)^{1-\frac{n_e}{n_r+1}}. \tag{S17}$$

In the last approximation, we have again assumed that the positions of the two genes along the chromosome are close. This expression indicates two cases, where gene

expression becomes independent of growth rate: (i) if n_e and n_r are the same and large, in that case expression of both the autorepressor R and the gene E exhibit no growth-rate dependence; and (ii) if $n_e=n_r+1$. In the latter case, R may have a weak growth-rate dependence, but expression of E becomes independent of the growth rate.

Autoactivation

An autoactivation circuit is described by

$$\dot{a} = a_1 F(\mu) A(a/K) - a. \tag{S18}$$

If a_1/K is small, the steady state concentration can be approximated by $a \approx a_1 F(\mu)/f$. In that limit, activation plays no role and the system is constitutively expressed. Likewise, for large a_1/K, expression is always fully activated and again essentially constitutive. In that case, we get $a \approx a_1 F(\mu)$.

For non-cooperative activation, i.e. if the activation function A has a Hill coefficient of $n=1$, intermediate values of a_1/K interpolate smoothly between these two limiting cases. For cooperative autoactivation, however, the steady state solution of Eq. (S18) goes through two saddle-node bifurcations and exhibits a region of bistability with two solutions that correspond to states of high and low expression of the autoactivator, respectively (see Fig. S3 A). A change of growth rate has two effects (compare the black and red curves for 1 and 2.5 doublings/hour): (i) The activator concentrations at low and high promoter strengths are reduced (by the same factor as constitutive expression, indeed the activator is effectively constitutively expressed in these regimes); and (ii) The region of bistability is shifted towards higher promoter strengths at faster growth, which is also seen from Fig. 6A.

The bifurcation points, i.e. the values of a_1/K at which bistability sets in, depend on the activation fold change as well as the Hill coefficient. In addition to a Hill coefficient >1,

bistability also requires a minimal activation fold-change ($f \gtrsim 9$ for n=2). The dependence on these parameters [obtained from linear stability analysis of Eq. (S18)] is shown by the 'phase diagram' in Fig. 6A. The lower boundary of the region of bistability depends only very weakly on f and n and is approximately given by $a_1/K \approx 2/F(\mu)$. The upper boundary however has a strong f-dependence and increase as $a_1/K \sim f^{(1-1/n)}/F(\mu)$ for large f. The increase of the exponent with increasing Hill coefficient n leads to an increase in the overlap area where bistability is obtained for a wider range of growth rates with increasing cooperativity.

Mutual repression toggle switch

The toggle switch circuits based on mutual repression of two genes R_1 and R_2 is described by two equations,

$$\dot{r}_1 = r_{1,1} F_1(\mu) R_1(r_2 / K_1) - r_1 \quad \text{(S19)}$$

$$\dot{r}_2 = r_{1,2} F_2(\mu) R_2(r_1 / K_2) - r_2. \quad \text{(S20)}$$

In these equations, both the growth functions F_1, F_2 and the repression functions R_1, R_2 for the two genes may have different parameters. We start however by considering the symmetric case, where all parameters are the same for both genes. For low values of $r_{1,1}/K_2 = r_{1,2}/K_1$, there is a unique solutions in the steady state, which correspond to constitutive expression with negligible repression, as the promoters are not strong enough to produce sufficient amounts of repressor to repress each other. For non-cooperative repression ($n_1 = n_2 = 1$), there is a smooth increase of the repressor concentration for all promoter strengths. For cooperative repression, the systems goes through a pitchfork bifurcation and exhibits bistability for large values of $r_{1,1}/K_2$. In that case, one of the two proteins is present at a high concentration and the other at a low concentration, shown by the upper and lower branches of the black and red curves in Fig. S3 B. As for the

autoactivator, the bifurcation point depends on the parameters of the repression function, which is shown in the 'phase diagram' in Fig. 6B.

Expression-dependent growth reduction

Next we consider a protein whose concentration p moderately inhibits growth. We take the growth rate to be reduced by a Hill-type function without cooperativity,

$$\mu(p/p_\mu) = \frac{\mu_{\max}}{1+p/p_\mu}. \qquad \text{(S21)}$$

As slower growth leads to a higher concentration of the protein, this represents a case of positive feedback. If the protein is expressed constitutively, its concentration in the steady state fulfills

$$p = p_1 F(\mu(p/p_\mu)). \qquad \text{(S22)}$$

If the growth-rate dependent factor $F(\mu)$ is given by the function for a chromosomal gene, this equation has one solution.

For genes on the plasmids pBR322 and R1, the growth-rate dependence (shown in Fig. 3C) can be approximated an exponential decrease $F(\mu)=(1/N)\exp(-\mu/\nu)$ with the normalization factor $N=\exp(-1\text{ dbl/hr}/\nu)$ and with $\nu\approx 0.75$ dbl/hr for pBR322 and $\nu\approx 0.5$ dbl/hr for R1. If we use $F(\mu)=(1/N)\exp(-\mu/\nu)$ in Eq. (S22), two solutions, and thus growth bistability, can be found in an intermediate range of the parameter p_1/p_μ, provided that ν is sufficiently small (for $\mu_0=2.5$ dbl/hr, $\nu<0.6$). The latter condition is satisfied for the R1 plasmid and growth bistability is predicted for this case (Fig. 7).

Autoactivator with growth-inhibition

Growth-mediated feedback can also work in conjunction with regulatory feedback. As an example we consider the autoactivator system described above, but now with the activator slowing down growth in a concentration-dependent manner described by Eq. (S21) above. In that case, the equation fulfilled by the concentration *a* of the autoactivator is Eq. (S18) supplemented by the *a*-dependent growth-rate, which leads to

$$a = a_1 F(\mu(a/a_\mu)) A(a/K), \tag{S23}$$

In this case the positive feedback due to autoactivation is supplemented by positive feedback arising from the growth reduction, and substantial expansion of the bistable regime may be expected; see Fig. S4. A similar effect has recently been discussed for an autoactivator system based on the T7 RNA polymerase (Tan & You, unpublished).

The expansion of the bistable region is reminiscent of the effect of increased cooperativity. Indeed, a simple analytical approximation shows that in this system the Hill coefficient of autoactivation is effectively increased by the additional positive feedback from growth reduction, provided that the concentration threshold for growth reduction is comparable to the concentration range for bistability in the corresponding autoactivator system without growth reduction. In that case we can approximate the activation function by $A(a) \approx (a/K)^n$ and the growth reduction by $\mu(a) \approx \mu_{max} K_\mu/a$. We further approximate $F(\mu) \sim \gamma/\mu$ with $\gamma = 1$ dbl/hr, which is a reasonable approximation for chromosomal genes if growth is not too slow, as discussed below. With these three approximations we obtain

$$a = a_1 \frac{a^{n+1}}{K^n K_\mu (\mu_{\max}/\gamma)}, \tag{S24}$$

which corresponds to autoactivation with an increase of Hill coefficient from *n* to *n*+1.

Repression with a basal level of expression

So far we have assumed that sufficiently high repressor concentrations can suppress expression of the repressed gene completely. Sometimes, however, a low basal level of gene expression can be observed even if very high repressor concentrations are present. There may be several sources of such basal level; one such source is given by transcription events that are initiated upstream of the promoter, presumably by initiation of transcription at a cryptic upstream promoter. The occurrence of such events is demonstrated by the fact that the basal level of expression of a repressed gene can be reduced appreciably (e.g., 10-fold) by inserting a strong terminator sequence upstream of the promoter (data not shown). In the following we show that the growth rate dependencies of circuits involving such a repressor are very similar to those for the corresponding circuit with perfect repression that has no basal level.

In this case, repression is described by the modified repression function

$$R(r/K) = \frac{1 + \frac{1}{f}(r/K)^n}{1 + (r/K)^n}, \qquad \text{(S25)}$$

which has one additional parameter, the fold-change f, which characterizes the ratio of the basal expression level to the expression level in absence of the repressor. The perfect repression case discussed so far is recovered for infinite f. The repression function now exhibits three different regimes:[1] For small repressor concentration, repression is negligible and expression is constitutive. Likewise, for large repressor concentrations, R is given by the fully repressed level (basal or leakage transcription), $R \sim 1/f$. We take this basal level to be constitutive as well, which should be correct for the case where transcription is initiated at cryptic upstream promoters. We note that other sources of basal expression could in principle exhibit different behavior. The typical repression case is obtained for intermediate repressor concentrations, such that $(r/K)^n$ is large compared to 1, but not $(r/K)^n/f$. In that case, we have $R \sim (K/r)^n$ and repression with a basal

[1] We note that the three regimes are only well separated for large repression fold-changes f, which is often the case.

expression level behaves just as repression without a basal expression level. This is shown in Fig. S5 A for the case of simple repression and in Fig. S5 B for autorepression. The data shown in these figures correspond exactly to the data shown in Fig. 4A and 5B, but now with a fold-change of $f = 1000$. Comparison of the figures shows that the same qualitative behavior is obtained for a small basal expression level and without basal expression, with only small quantitative differences between the two cases.

In the case of the toggle switch of two repressors that mutually repress each other, the existence of a basal expression level has the effect that bistability disappears again (through a second pitchfork bifurcation) for very high promoter strengths, as shown in Fig. S5 C, similar to the autoactivator case (Fig. 6A, but we note that formally the two systems are different and exhibit different types of bifurcations), but different from the toggle switch systems based on repressors without a basal expression level (Fig. 6B), where bistability persists for all sufficiently large promoter strengths. As shown in Fig. S5 C, there are unique solutions in the steady state for low and high values of $r_{1,1}/K_2=r_{2,1}/K_2$, which correspond to constitutive expression with either negligible repression and to basal (fully repressed) expression of the genes. As a consequence, for repressors with a basal level, the existence of bistability at the fastest growth therefore does not guarantee the existence of bistability at all growth rates, as in the case without a basal expression level. This is shown by the 'phase diagram' in Fig. S5 D (for the symmetric case where both repressors are characterized by the same parameters), which resembles the one for the autoactivator system (Fig. 6A). For very strong promoters it is possible that bistability occurs at fast growth, but not at slower growth. However, the promoter strength required for this case increases strongly with the fold change f (the f-dependence of the upper boundary of the phase diagram depends on the Hill coefficient, ut in general exhibits a faster than linear increase). Therefore the overlap region (grey area), where bistability is obtained over a wide range of growth rates, is much larger than for the autoactivator. If we consider further that for real repressors the basal level should be low and thus that the fold-change f is large, we expect the case that such a system is bistable at fast growth, but not slow growth to be very rare, so that practically it should be

enough to require bistability at the fastest growth rate to obtain bistability also at slow growth, as in the case without a basal expression level.

Supporting experimental methods

Strain construction

Strains and the plasmids used for strain construction are described in Table S1. Oligonucleotides used in this study are described in Table S2. All the strains used were derived from *E. coli* K12 strain MG1655 that was kindly provided by F. R. Blattner (University of Wisconsin).

To avoid the possible effect of expression of the *lacY* gene driven by a foreign promoter on bacterial growth or inducer uptake, the gene was deleted without anything left behind using a recombineering protocol involving the *galK* positive selection and counterselection (Warming et al., 2005). Basically, the *galK* gene was deleted by the method of Datsenko and Wanner (2000) using primers GalK1-P1 and GalK2-P2 (Table S2). The resultant strain lost the ability to grow on galactose. The *galK* gene together with a constitutive promoter was amplified from pgalk (Warming et al., 2005) using primers GalK1-lacY1 and GalK2-lacY2, each of which is composed of a 20 bp region at the 3' end that is complementary to the *galK* sequence, and a 50 bp region at the 5' end that is homologous to the *lacY* gene. The PCR products were gel purified using an EZ gene^{TM} Gel Extraction kit (Biomiga), treated with *Dpn*I, and then electroporated into MG1655 (EQ1) cells that expressed the lambda-Red proteins encoded by plasmid pKD46. The pKD46 plasmid, which carries a temperature-sensitive origin of replication, was removed by growing the mutant cells overnight at 40 ^{o}C. The cells were applied onto minimal M63 agar plates with galactose (0.5%. w/v) as the sole carbon source. The Gal^{+} mutants were purified on new M63 + galactose plates and verified for the replacement of *lacY* by *galK* using PCR and subsequent DNA sequencing. Two 100 bp DNA oligos that are complementary each other were synthesized, each of which contains a 50 bp region at

the 5'end that is homologous to the immediate upstream region of the *lacY* deletion, and a 50 bp region at the 3' end that is homologous to the immediate downstream of the *lacY* deletion. These two oligos were annealed together and the resultant double-stranded DNA fragments were electroporated into the cells of a Gal^+ mutant in which *galK* was substituted for *lacY*. The cells were applied onto minimal M63 agar plates with glycerol and 2-deoxygalactose (a galactose analog that is toxic when it is phosphorylated by GalK). The growth-positive, deoxygalactose-resistant mutants, in which the *galK* gene in the *lacY* locus was supposed to be replaced by the double-stranded oligos, were purified on the same plates and verified by PCR and DNA sequencing. The final mutant, designated as EQ42, therefore contained the seamless deletion of the *lacY* gene.

To construct a strain (EQ37) in which the native chromosomal *lacZ* gene is driven by a synthetic promoter repressible by TetR, the $P_{LTet\text{-}O1}$ promoter plus the ribosome binding site was cloned from pZA31-*luc* (Lutz and Bujard, 1997) into the *Sal*I and *BamH*I sites of pKD13 (Datsenko and Wanner, 2000). Upstream of $P_{LTet\text{-}O1}$ in pKD13 is a FRT-flanking *km* gene. To block any possible transcription from the upstream regions, an *rrnB* terminator (*rrnB*T) was amplified, digested with *Sal*I and *Xho*I, and ligated into the same sites of pKD13 carrying $P_{LTet\text{-}O1}$, yielding pKD13-*rrnB*T:$P_{LTet\text{-}O1}$, which therefore contains the terminator immediately upstream of $P_{LTet\text{-}O1}$. The resultant *km*:*rrnB*T:$P_{LTet\text{-}O1}$ was amplified using primers Ptet1-P1 and Ptet2-P2 (Table S3). Ptet1-P1 contains a 50 bp region that is homologous to the *lacI* promoter region while Ptet2-P2 contains a 50 bp region that is homologous to the first 50 bp region of the *lacZ* structural gene. The PCR products were gel purified, treated with *Dpn*I, and then electroporated into EQ42 cells that expressed the lamda-Red proteins. The cells were applied onto LB + km agar plates. The kanamycin resistant mutants were verified for the substitution of *km*:*rrnB*T:$P_{LTet\text{-}O1}$ for the *lacI* gene and the native *lacZ* promoter by PCR and subsequent DNA sequencing. Similar methods were used to construct strain EQ48, in which the P*u* promoter (Perez-

Martin and de Lorenzo, 1996) was integrated to replace the *lacI* gene and the native *lac* promoter, thereby driving *lacZ* at the *lac* locus. No terminator was placed upstream of the P*u* promoter since this promoter has been reported to be able to block transcription from its upstream DNA region (Velazquez et al., 2006).

To make strain EQ43, the Pcon-*tetR* construct (in which *tetR* is driven by a constitutive promoter) was amplified from pZsin4-1 (Lutz and Bujard, 1997), digested with *Sac*I and *BamH*I, and ligated into the same sites of pLDR10, a chromosomal integration vector (Diederich et al., 1992). The resultant plasmid was digested with *Not*I and the fragments were separated by gel eletrophoresis. The larger DNA fragment containing the Pcon-*tetR* construct, the *attP* region and the *bla* gene was self-ligated and then transformed to EQ42 cells that expressed the integrase encoded by pLDR8 (Diederich et al., 1992). The cells were plated on LB + Ap agar plates that were then incubated at 42 ^{o}C (to facilitate integration and to lose pLDR8 that contains a temperature-sensitive *ori*). The Ap^{r} colonies were purified, and then confirmed for the integration of both the Pcon-*tetR* and the *bla* gene into the *attB* site as described in Diederich et al. (1992).

To make EQ44, the *tetR* structural gene was first substituted for the *luc* gene in pZA31-*luc* (Lutz and Bujard, 1997). The resultant plasmid contains the synthetic $P_{LTet\text{-}O1}$ driving *tetR*. The $P_{LTet\text{-}O1}$-*tetR* construct was ligated to pLDR10 and then integrated into the *attB* site as above (Diederich et al., 1992). To make strain EQ45, the wild type *xylR* gene (Perez-Martin and de Lorenzo, 1996) was deleted of the first 675 bps from the 5' end, resulting in a shorter version of the gene (*dnxylR*) that encodes a constitutively active activator of the P*u* promoter. The *dnxylR* gene was substituted for *gfp* in pZE12-*gfp* (Levine et al., 2007). The $P_{Llac\text{-}O1}$-*dnxylR* from the resultant plasmid was cloned into pLDR10 and subsequently integrated to the *attB* site (Diederich et al., 1992).

The other strains listed in Table S1 (EQ38, EQ39 and EQ40) were made via P1 transduction by combining two respective constructs together in the EQ42 strain background. All the constructs were confirmed by DNA sequencing.

Bacterial media and growth

For DNA manipulations such as strain construction and P1 transduction, E. coli strains were regularly cultured in LB at 37ºC or 30ºC. When appropriate, kanamycin (Km; 25 μg/ml), ampicillin (Ap; 100 μg/ml), or chloromphenicol (25 μg/ml) was added to the media.

To culture the strains at different growth rates (ranging from ~0.3 to ~2.5 doublings per hour), five defined media were chosen for bacterial growth. These defined media were basically derived from M63 minimal medium (Miller, 1972) and rich defined medium (RDM) (Neidhardt et al., 1974). Glycerol or glucose was added at 0.5% (w/v) to the media as the primary carbon source. For M63 minimal media, 20 mM ammonia (NH_4) or 20 mM glycine serves as the nitrogen source. These five media are 1) RDM + glucose; 2) RDM + glycerol; 3) M63 + NH_4 + glycerol + casamino acids (0.2%); 4) M63 + NH_4 + glycerol; and 5) M63 (no NH4) + glycerol + glycine (20 mM, the sole nitrogen source).

Measurements of growth rate, total protein and β-galactosidase activity

To measure growth rates, test strains were first cultured in LB for ~5 hours. The LB cultures were inoculated to defined measurement media. When OD600 reached 1.5 to 2, the cultures (pre-cultures) were inoculated to 5 ml of the same media (measurement media) in sterile glass tubes (20 mm x 150 mm) at initial OD600 = 0.01. No antibiotic was added to any of the measurement media. For strains EQ38 and EQ39, chloro-

tetrocycline (Sigma) was added to the measurement media at 0, 20, 50 ng/ml. The tubes were incubated with shaking (250 rpm) at 37°C in a waterbath shaker. After growth for at least two generations, samples were taken for measurements of OD_{600}, total protein amounts, and β-galactosidase activities. OD_{600} was measured using a Bio-Rad spectrophotometer. The total proteins were measured using the Micro Lowry Total Protein kit from Sigma and normalized to μg per milliliter. For β-galactosidase aaasy, four samples from each growing culture were collected during the exponential growth (OD_{600} = 0.1 to ~1). For each sample, the total protein level (μg/ml) and the LacZ level (ΔOD_{420}/min/ml) were measured. The LacZ activity per total protein was obtained as the slope of the plot of LacZ activity levels vs total protein levels. The LacZ activity per cell mass was obtained as the slope of the plot of LacZ activity levels vs OD_{600}.

REFERENCES

Bernstein, J.A., Khodursky, A.B., Lin, P.H., Lin-Chao, S., and Cohen, S.N. (2002). Global analysis of mRNA decay and abundance in Escherichia coli at single-gene resolution using two-color fluorescent DNA microarrays. Proc Natl Acad Sci U S A *99*, 9697-9702.

Bintu, L., Buchler, N.E., Garcia, H.G., Gerland, U., Hwa, T., Kondev, J., and Phillips, R. (2005). Transcriptional regulation by the numbers: models. Curr Opin Genet Dev *15*, 116-124.

Bipatnath, M., Dennis, P.P., and Bremer, H. (1998). Initiation and velocity of chromosome replication in Escherichia coli B/r and K-12. J Bacteriol *180*, 265-273.

Bremer, H., and Dennis, P.P. (1996). Modulation of chemical composition and other parameters of the cell by growth rate. In Escherichia coli and Salmonella, F.C. Neidhardt, ed. (Washington D.C., ASM Press), pp. 1553-1569.

Brunschede, H., Dove, T.L., and Bremer, H. (1977). Establishment of exponential growth after a nutritional shift-up in Escherichia coli B/r: accumulation of deoxyribonucleic acid, ribonucleic acid, and protein. J Bacteriol *129*, 1020-1033.

Cai, L., Friedman, N., and Xie, X.S. (2006). Stochastic protein expression in individual cells at the single molecule level. Nature *440*, 358-362.

Cayley, S., and Record, M.T. (2004). Large changes in cytoplasmic biopolymer concentration with osmolality indicate that macromolecular crowding may regulate protein-DNA interactions and growth rate in osmotically stressed Escherichia coli K-12. Journal of Molecular Recognition *17*, 488-496.

Cole, J.R., Olsson, C.L., Hershey, J.W., Grunberg-Manago, M., and Nomura, M. (1987). Feedback regulation of rRNA synthesis in Escherichia coli. Requirement for initiation factor IF2. J Mol Biol *198*, 383-392.

Datsenko, K.A., and Wanner, B.L. (2000). One-step inactivation of chromosomal genes in Escherichia coli K-12 using PCR products. Proc Natl Acad Sci U S A *97*, 6640-6645.

Dennis, P.P., and Bremer, H. (1974). Macromolecular composition during steady-state growth of Escherichia coli B-r. J Bacteriol *119*, 270-281.

Diederich, L., Rasmussen, L.J., and Messer, W. (1992). New cloning vectors for integration in the lambda attachment site attB of the Escherichia coli chromosome. Plasmid *28*, 14-24.

Donachie, W.D., and Robinson, A.C. (1987). Cell division: Parameter values and the process. In Escherichia coli and Salmonella typhimurium, F.C. Neidhardt, J.L. Ingraham, B. Magasanik, K.B. Low, M. Schaechter, and H.E. Umbarger, eds. (Washington DC, ASM), pp. 1578-1592.

Elf, J., Li, G.W., and Xie, X.S. (2007). Probing transcription factor dynamics at the single-molecule level in a living cell. Science *316*, 1191-1194.

Elowitz, M.B., Surette, M.G., Wolf, P.E., Stock, J.B., and Leibler, S. (1999). Protein mobility in the cytoplasm of Escherichia coli. J Bacteriol *181*, 197-203.

Engberg, B., and Nordstrom, K. (1975). Replication of R-factor R1 in Escherichia coli K-12 at different growth rates. J Bacteriol *123*, 179-186.

Jain, C., and Belasco, J.G. (1995). RNase E autoregulates its synthesis by controlling the degradation rate of its own mRNA in Escherichia coli: unusual sensitivity of the rne transcript to RNase E activity. Genes Dev *9*, 84-96.

Jain, C., Deana, A., and Belasco, J.G. (2002). Consequences of RNase E scarcity in Escherichia coli. Mol Microbiol *43*, 1053-1064.

Jinks-Robertson, S., Gourse, R.L., and Nomura, M. (1983). Expression of rRNA and tRNA genes in Escherichia coli: evidence for feedback regulation by products of rRNA operons. Cell *33*, 865-876.

Keener, J., and Nomura, M. (1996). Regulation of ribosome synthesis. In Escherichia coli and Salmonella, F.C. Neidhardt, ed. (Washington D.C., ASM Press), pp. 1417-1431.

Klumpp, S., and Hwa, T. (2008). Growth-rate-dependent partitioning of RNA polymerases in bacteria. Proc Natl Acad Sci U S A *105*, 20245-20250.

Kushner, S.R. (2007). Messenger RNA decay. In EcoSal - Escherichia Coli and Salmonella, A. Böck, R. Curtiss III, J.C. Kaper, P.D. Karp, F.C. Neidhardt, T. Nystrom, J.M. Slauch, C.L. Squires, and D. Ussery, eds. (Washington, DC, ASM Press).

Lawrence, J.V., and Maier, S. (1977). Correction for the inherent error in optical density readings. Appl Environ Microbiol *33*, 482-484.

Levine, E., Zhang, Z., Kuhlman, T., and Hwa, T. (2007). Quantitative characteristics of gene regulation by small RNA. PLoS Biol *5*, e229.

Liang, S.T., Bipatnath, M., Xu, Y.C., Chen, S.L., Dennis, P., Ehrenberg, M., and Bremer, H. (1999a). Activities of constitutive promoters in Escherichia coli. J Mol Biol *292*, 19-37.

Liang, S.T., Ehrenberg, M., Dennis, P., and Bremer, H. (1999b). Decay of rplN and lacZ mRNA in Escherichia coli. J Mol Biol *288*, 521-538.

Liang, S.T., Xu, Y.C., Dennis, P., and Bremer, H. (2000). mRNA composition and control of bacterial gene expression. J Bacteriol *182*, 3037-3044.

Lin-Chao, S., and Bremer, H. (1986). Effect of the bacterial growth rate on replication control of plasmid pBR322 in Escherichia coli. Mol Gen Genet *203*, 143-149.

Lutz, R., and Bujard, H. (1997). Independent and tight regulation of transcriptional units in Escherichia coli via the LacR/O, the TetR/O and AraC/I1-I2 regulatory elements. Nucleic Acids Res *25*, 1203-1210.

Maaløe, O. (1979). Regulation of the protein-synthesizing machinery - ribosomes, tRNA, factors, and so on. In Biological regulation and development, R.F. Goldberger, ed. (New York, Plenum Press), pp. 487-542.

Miller, J.H. (1972). Experiments in Molecular Genetics (Cold Spring Harbor, NY, Cold Spring Harbor Laboratory).

Mudd, E.A., and Higgins, C.F. (1993). Escherichia coli endoribonuclease RNase E: autoregulation of expression and site-specific cleavage of mRNA. Mol Microbiol *9*, 557-568.

Nanninga, N., and Woldringh, C.L. (1985). Cell growth, genome duplication, and cell division. In Molecular cytology of Escherichia coli, N. Nanninga, ed. (London, Academic Press), pp. 259-318.

Neidhardt, F.C., Bloch, P.L., and Smith, D.F. (1974). Culture medium for enterobacteria. J Bacteriol *119*, 736-747.

Nilsson, G., Belasco, J.G., Cohen, S.N., and von Gabain, A. (1984). Growth-rate dependent regulation of mRNA stability in Escherichia coli. Nature *312*, 75-77.

Ow, M.C., Liu, Q., Mohanty, B.K., Andrew, M.E., Maples, V.F., and Kushner, S.R. (2002). RNase E levels in Escherichia coli are controlled by a complex regulatory system that involves transcription of the rne gene from three promoters. Mol Microbiol *43*, 159-171.

Ozbudak, E.M., Thattai, M., Kurtser, I., Grossman, A.D., and van Oudenaarden, A. (2002). Regulation of noise in the expression of a single gene. Nature Genetics *31*, 69-73.

Perez-Martin, J., and de Lorenzo, V. (1996). In vitro activities of an N-terminal truncated form of XylR, a sigma 54-dependent transcriptional activator of Pseudomonas putida. J Mol Biol *258*, 575-587.

Schaechter, M., Maaløe, O., and Kjeldgaard, N.O. (1958). Dependency on medium and temperature of cell size and chemical composition during balanced growth of Salmonella typhimurium. J Gen Microbiol *19*, 592-606.

Scott, M., Gundersen, C.W., Mateescu, E., Zhang, Z., and Hwa, T. (2009). Growth laws and proteome partition dictate the growth dependence and fitness cost of bacterial gene expression. in submission.

Velazquez, F., Fernandez, S., and de Lorenzo, V. (2006). The upstream-activating sequences of the sigma54 promoter Pu of Pseudomonas putida filter transcription readthrough from upstream genes. J Biol Chem *281*, 11940-11948.

Warming, S., Costantino, N., Court, D.L., Jenkins, N.A., and Copeland, N.G. (2005). Simple and highly efficient BAC recombineering using galK selection. Nucleic Acids Res *33*, e36.

Woldringh, C.L., Binnerts, J.S., and Mans, A. (1981). Variation in Escherichia coli buoyant density measured in Percoll gradients. J Bacteriol *148*, 58-63.

Zimmerman, S.B., and Trach, S.O. (1991). Estimation of Macromolecule Concentrations and Excluded Volume Effects for the Cytoplasm of Escherichia Coli. J Mol Biol *222*, 599-620.